# Secondary Ion Mass Spectrometry

# SIMS VIII

Proceedings of the Eighth International Conference on
**Secondary Ion Mass Spectrometry (SIMS VIII)**

International Congress Centre RAI, Amsterdam, The Netherlands
September 15–20th, 1991

Editors
A. Benninghoven · K.T.F. Janssen · J. Tümpner · H.W. Werner

JOHN WILEY & SONS
*Chichester · New York · Brisbane · Toronto · Singapore*

# STATE–SELECTED STUDIES OF ATOMS AND MOLECULES EJECTED FROM ION BOMBARDED SURFACES

Nicholas Winograd

The Pennsylvania State University, Department of Chemistry, 152 Davey Laboratory,
University Park, PA 16802, USA

## I. Introduction

A fundamental understanding of the essential physics which contributes to the formation of secondary ions requires a global view of the energy transfer processes which occur subsequent to the ion bombardment event. Many different pathways are known which must contribute to this global view including the desorption of ground state and excited state neutral atoms, desorption of molecules and clusters in various rotation and vibrational excited states, and desorption of species induced by electronic transitions. In many experimental configurations the SIMS component is a minor fraction of the total possible energy–loss pathways.

During recent years, new experimental and theoretical approaches have emerged which allow detailed studies of the energy and angular neutral (EARN) distributions of atomic and molecular species as they leave the surface.[1] These types of studies are crucial for evaluating the efficacy of proposed theoretical models since it is much more difficult to predict the detailed particle motion than it is to predict total yields. The models themselves have evolved from the early formalisms of Thompson and Sigmund which employed the binary collision approximation (BCA) and energy transport equations. Computer simulations of the classical motion began by using the BCA but rapidly grew in accuracy by incorporating more sophisticated interaction potentials using microcrystallites containing 2000 atoms or more. Modern computers can now handle many–body potential functions based on the embedded atom method for metal targets[2] and potentials which incorporate directional bonding for covalent solids such as Si.[3] In our laboratory, it is now possible to accurately measure these distributions for ground state neutral atoms using a highly selective and sensitive multiphoton resonance ionization detector. Moreover, using complementary technology, we can obtain these distributions for excited states, secondary ions, and a selected set of desorbed molecular species.

In this paper, three examples will be given which illustrate our efforts to obtain the global view we deem to be necessary to fully appreciate the ion/solid interaction. These include (i) a first report of the energy and angular distributions of excited Rh atoms from the Rh{100} surface, (ii) an example using NaCl{100} of how electronic effects can complicate desorption by collision cascades and (iii) a

techniques have advanced considerably in their capability over the last decade and that it is now feasible to obtain detailed information about the desorbed species. Although these experiments are certainly not routine or trivial, the results are beginning to impact our understanding of this complex phenomenon.

## II. Experimental

We have employed multiphoton resonance ionization (MPRI) spectroscopy as a state–selective probe to monitor the trajectory of ground and excited–state species. Briefly, the measurements are performed in an ultra–high vacuum chamber ($2x10^{-10}$ Torr base pressure) equipped with LEED and Auger spectroscopy.[4] The experiment proceeds as follows. A 200–nsec pulse of 5 keV $Ar^+$ is focused, at normal incidence, onto a 2–mm spot on the sample. A given time after the ion impact, a ribbon–shaped laser pulse (1 mJ for 6 nsec) is used to ionize a small volume of the desorbed particles, thus defining the time of flight (TOF) of the probed species. The MPRI technique is employed to selectively ionize the ejected particles. Once the particles are ionized, they are accelerated toward a position–sensitive microchannel plate detector and are displayed on a phosphor screen located in the back of it. The image is, in–turn, monitored by a charge–coupled–device camera which is interfaced to a micro–VAX station II for data storage and processing. For a typical spectrum, 30 to 60 images, each corresponding to a different TOF, are collected and sorted into an intensity map of kinetic energies and takeoff angles.

For the NaCl experiments, an optical quality NaCl{100} crystal was cleaved in air and subsequently cleaned by heating to 660 K in ultra–high vacuum for several hours. This procedure produces well ordered, single crystal surfaces as examined by LEED.

## III. Results and Discussion

### A. Rh($^4F_{9/2}$) and Rh($^4F_{7/2}$) EARN distributions from Rh{100}.

The energy– and angle–resolved distributions of Rh atoms sputtered in the ground state and the next higher–lying excited state are presented in Fig. 1. The results correspond to ejection along two crystallographic directions, as defined in the inset to Fig. 1. For the ground state distribution, the most intense peak is seen along the $\varphi = 0°$ azimuth (<100> direction) at a polar angle of about 50°. The observed angular anisotropies are the same as has been reported previously for the ground state.[5] The EARN distributions of excited atoms ($^2F_{7/2}$) exhibit several features that are qualitatively different from the ground state ($^2F_{9/2}$) distributions. First, the most intense peak appears at normal ejection ($\theta$=0°). Second, at low energies, only a shoulder exists along the $\varphi = 45°$ azimuth (<110> direction). Third, the off–normal peak position occurs closer to the surface normal for the excited state than for the ground state. Fourth, the fall–off with energy is much slower for the excited state.[6]

Over the years, the excitation probability has been defined in various ways and has been related to the expression $\exp(-A/av_\perp)$.[7] Assuming that the population of the excited state by cascading from higher lying states are insignificant in our measurements, the excitation probability is the ratio of the excited state population to the total population. This latter quantity, however, is generally inac-

cessible experimentally since the total yield of atoms and molecules in all electronic states cannot be measured. Since in our case the $^4F_{7/2}$ excited species are only ~5% of the ground state atoms, we approximate the excitation probability by the ratio of the excited state population to the ground state population. This, in turn, is proportional to the ratio of the excited state to the ground state distributions, (dN*/dv)/(dN/dv), which is presented in Fig. 2 as a function of $1/v_\perp$ for a few representative angles of ejection.

There are several remarkable features that are clear from inspection of Fig. 2. First, at high velocities the ratio exhibits the expected $\exp(-A/av_\perp)$ dependence. Unexpectedly, however, the value of A/a varies from $0.58 \times 10^6$ to $1.52 \times 10^6$ cm/s. Second, at low velocities there is a sharp leveling off of the intensity ratios. The height of this plateau depends strongly on the polar and azimuthal angles of ejection. A somewhat similar behavior has been observed and attributed to the effect of surface binding energy.[8] However, in the present investigation, the deviation at low velocities occurs much more abruptly, suggesting the existence of an additional excitation mechanism.

We are currently attempting to unravel the significance of this observation. Briefly, we have attempted to model the excitation event using collisional excitation which can be incorporated into the classical dynamics computer simulations. The results show that the leveling off arises from three separate factors. These are (i) the presence of the $e^{-1/v_\perp}$ decay rate, (ii) the presence of a set of excitations that occur with 5–20 Å of the surface. Within the framework of the model, these atoms are far removed from interaction of the substrate, and thus their lifetimes are much longer. And (iii), the presence of microscopic collision sequences within the cascade. For example, two atoms ejected at different angles can have different trajectory histories and different final excitation probabilities, yet emerge with the same final value of $v_\perp$. Moreover, at high energies and off–normal angles ($\theta$>30°), an exciting atom can get reexcited via a collision with a neighboring atom. This leads to the observed angular variations of a/A.

The implications of these results may well apply to the ejection of ions from keV particle bombarded clean metals. Collisional effects would lead to a non–$\exp(-A/av_\perp)$ velocity dependence of the ionization probability at low velocity, thus explaining experimental data which indicate the dependence should be $V^n$ where n=0–2. The collisions of particles over the surface may also explain why calculated ion fractions for clean metals are often many orders of magnitude smaller than those measured experimentally.

B. Electronic and Nuclear Effects in Ion–Induced Desorption from NaCl{100}.

Electronic excitations may occur via collisions or via the presence of electrons. For alkali halides, the first step is the conversion of energy deposited into the electronic system of the crystal by formation of self–trapped exciton (STE). The nonradiative decay of the STE into a halogen vacancy (F center) and an interstitial halogen atom (H center) leads to desorption. Williams et al. have distinguished be-

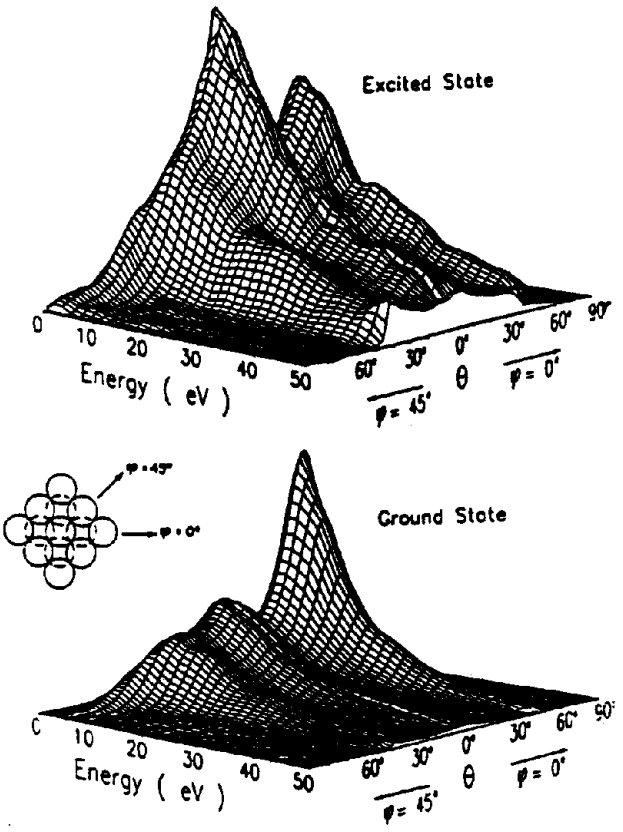


Fig. 1. Energy– and angle–resolved distributions of Rh atoms in the $^4F_{7/2}$ excited state and $^4F_{9/2}$ ground state, ejected from 5 keV $Ar^+$ ion bombarded Rh{100}. The data correspond to ejection along φ=0° (<100>) and φ=45° (<110>) crystallographic directions, as defined in the inset. Due to the symmetry of the surface and the angular resolution (Δφ=±10°), the results represent the behavior over ~50% of all space. Both plots are normalized to the maximum intensity peaks.

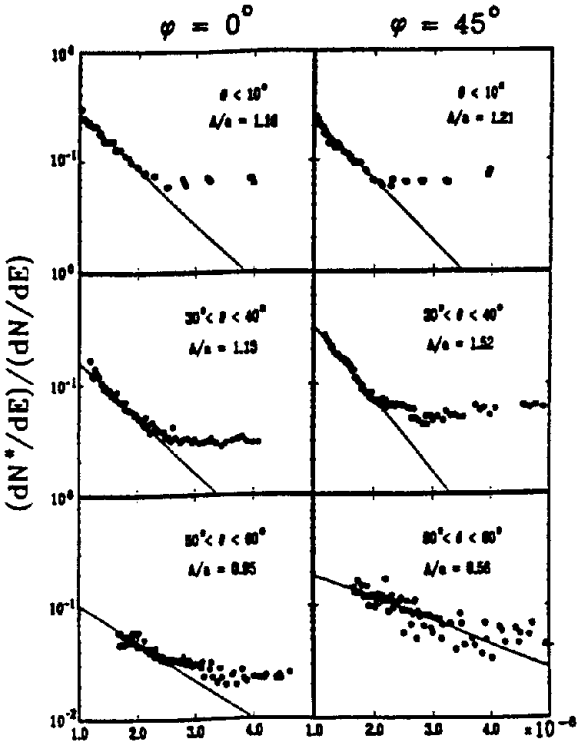


Fig. 2. Ratio of the measured intensities, (dN*/dV)/(dN/dV), vs $1/v_\perp$ for different angles of ejection. The data are direct ratios of the intensities given in Figure 1. Straight lines have been fit to the high velocity portions of the data and have slopes, A/a, (in units of $10^6$ cm/s) as displayed in each frame.

out of the relaxed STE in its lowest $\pi$–luminescence state. This process ends by the thermal evaporation of the diffusing neutral halogen atom. In the dynamic process, the energy of the F–H pair formation is derived from the energy stored in the higher excitonic state of the STE. If such an event occurs in close proximity to the surface, it can lead to the emission of a non–thermal halogen atom. If, instead, the dynamic process occurs deeper in the bulk, it produces an H center which can reach the surface by thermal diffusion, and contribute to the thermal emission. The desorption of the halogen atoms by these two processes leads to the formation of a surface layer enriched in alkali ions. These ions can subsequently be neutralized by secondary electrons or by recombining with the F centers.[10] Since neutral alkali atoms are loosely bound to the surface, they simply evaporate.

It has been reported that Na atoms ejected from ion–bombarded NaCl single crystals have only a thermal distribution.[11,12] These results are in contradiction with the earlier measurements on polycrystalline samples where significant collisional contribution was observed.[13] To help resolve this discrepancy, the TOF distributions of Na atoms emitted from an ion–bombarded NaCl{100} surface at several target temperatures have been measured. For these investigations, a 5 keV $Ar^+$ ion beam at normal incidence is employed, and only particles ejected along the <111> crystallographic direction are collected. Two components are visible in the spectra. The distributions at small TOF can be described by a Thompson formula with a surface binding energy of about 1.5 eV which indicates that particles contributing to this part of the spectrum originate from the collision cascade.[13] Moreover, this component appears not to depend on the target temperature. In contrast, the feature appearing at $t>5$ μs is very sensitive to the temperature of the sample. For temperatures higher than 100°C, this part of the spectrum can be described by the Maxwell–Boltzmann distribution.

By integrating the areas under the curves of these measurements, the dependence of the thermal and collisional components on the target temperature can be determined. As is shown in Fig. 3, the yield is already saturated at 80°C. This contradicts the previous experiments with Ar ions and electrons, in which the plateau was not reached even at 200°C.[11,14] The beam–induced changes in surface stoichiometry are potentially responsible for this discrepancy. In the previous measurements, the surface was bombarded by a continuous beam with an average fluence of $10^{15}$–$10^{17}$ ions/cm$^2$. In electron bombardment experiments, it is shown that a high incident dose leads to a surface layer enriched in Na.[14] In this case, the emission of Na atoms is controlled more by the evaporation rate of the alkali atoms than by the rate of defect creation. In our measurements, the total dose is less than $10^{13}$ ions/cm$^2$ ($2\times10^6$ ions/cm$^2$ in a 150 ns pulse). Under these conditions, the balance between the rate of evaporation and the rate of defect formation can be reached at much lower temperatures.

The collisional contribution obtained in our measurements is still considerably smaller than reported on compressed–powder targets. One phenomenon that would explain this discrepancy is the channeling of the incident beam. This hypothesis can be verified by investigating the dependence of the TOF distribution on the azimuthal direction of the incident beam. As shown in Fig. 4, we have exam-

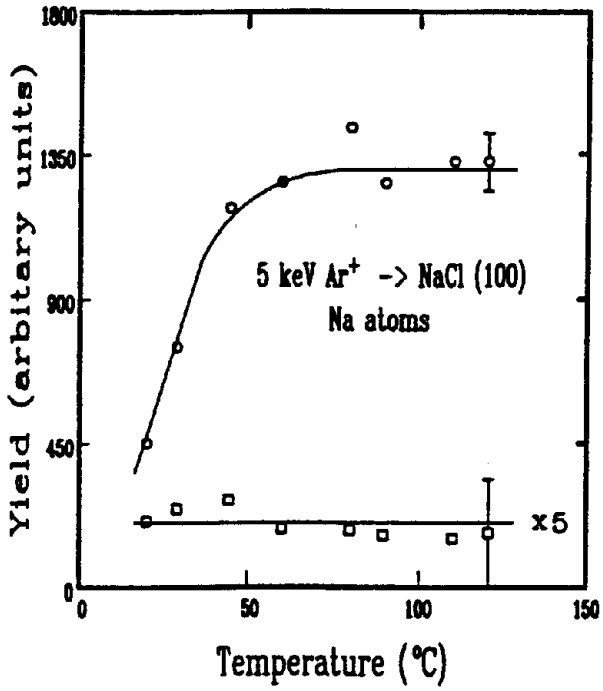


Fig. 3. The dependence of the thermal (O) and the collisional (□) contributions on the target temperature. The solid line is drawn only as an aid to the eye.

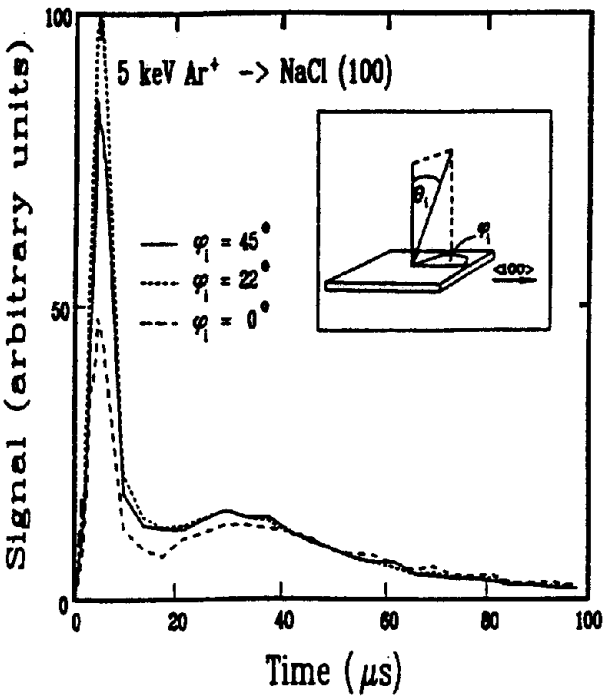


Fig. 4. The TOF distributions of Na atoms emitted from ion bombarded NaCl{100} surface. The target is held at 20°C. The spectra correspond to three different azimuthal directions $\varphi_i$ of the incident 5 keV Ar+ beam. The polar angle of incidence $\theta_i$ is fixed to be 45° with respect to the surface normal. Only particles emitted perpendicular to the surface are recorded. Spectra are not normalized.

ined a geometry where the polar angle of incidence is fixed at 45° with respect to the surface normal, and the azimuthal angle of incidence, $\varphi_i$, is varied. The target is held at room temperature, and only Na atoms ejected perpendicular to the surface are recorded. The resulting spectra for $\varphi_i$=0° (<101>), $\varphi_i$=45° (<111), and $\varphi_i$=22° are then recorded. In a cubic lattice, these directions correspond to different degrees of "openness", ranging from very open for $\varphi_i$=0° to nearly random for $\varphi_i$=22°. Compared to the spectra taken at normal ion incidence, the present geometry enhances the collisional component relative to the thermal contribution. Furthermore, the ratio of the collisional yield to the thermal yield depends on the azimuthal angle of incidence and is maximum at $\varphi_i$=22°.

C. Characterization of Molecular Clusters.

The ejection mechanisms of clusters in an ion bombardment process has been of long–standing interest.[15] For the NaCl system, the neutral mass spectrum indicates a significant emission of $Na_2$ dimers. To determine its mechanism of emission, multiphoton resonant ionization spectroscopy can be employed to measure the TOF distribution of $Na_2$. Although we tuned the laser wavelength to a known $Na_2$ transition, and the frequency scan of the ionizing radiation showed a very broad, multicomponent absorption band, no signal at the mass of $Na_2$ was observed. Instead, a very strong signal is present at the mass of atomic Na indicating that all the $Na_2$ dimers are photo–fragmented during the ionization process.

The TOF distribution of Na produced by photo–fragmentation of $Na_2$ is shown in Fig. 5. In the same figure, the TOF spectrum of neutral Na atoms is presented. For these measurements, the target is held at 130°C. Surprisingly, the two distributions look strikingly similar. It has been suggested that halogen molecules ejected by electron or ion bombardment are created by the recombination of halogen atoms at the crystal surface.[16] However, this model cannot explain our data. If $Na_2$ dimers are created at the surface, they must have the same energy spectrum as Na atoms. Since the mass of $Na_2$ is twice the mass of atomic Na, the TOF distribution of $Na_2$ must, in this case, be shifted towards longer times. Since the monomer and the dimer TOF spectra are similar, the $Na_2$ must be formed above the original surface plane, but still within the interaction range of the solid in order for the excess kinetic energy to be removed.[15]

## Acknowledgement

I would like to thank my numerous colleagues for their collaborations including B. Garrison, Z. Postawa, R. Maboudian, M. El–Maazawi, M. Ervin, M. Wood and D. Bernardo. In addition, I wish to thank NSF, ONR and DOE for generous financial support.

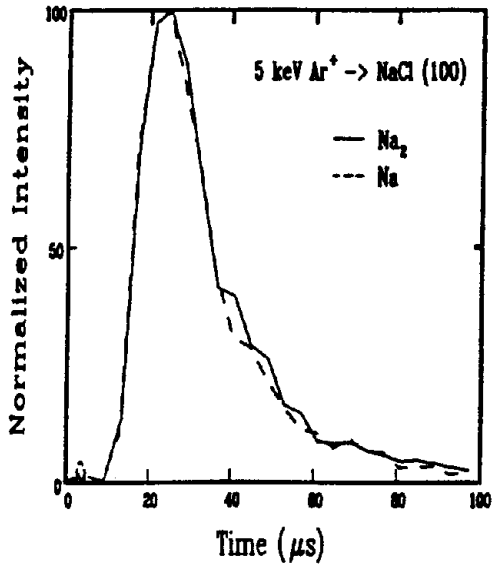


Fig. 5. The TOF distributions of $Na_2$ dimers (solid line) and Na atoms (dashed line) emitted from ion bombarded NaCl{100} at 130°C.

**References**


1. N. Winograd and B. J. Garrison in "Methods of Surface Characterization", Vol. 2, ed. D. Hercules and A. Czanderna, Plenum, NY (1991).
2. B. J. Garrison, N. Winograd, D. M. Deaven, C. T. Reimann, D. Y. Lo, T. A. Tombrello, D. E. Harrison, Jr. and M. H. Shapiro, Phys. Rev. B 37, 7197 (1988).
3. R. Smith, D. E. Harrison, Jr. and B. J. Garrison, Phys. Rev. B 40, 93 (1989).
4. P. H. Kobrin, G. A. Schick, J. P. Baxter and N. Winograd, Rev. Sci. Instrum. 57, 1354 (1986).
5. R. Maboudian, Z. Postawa, M. El–Maazawi, B. J. Garrison and N. Winograd, Phys. Rev. B 42, 7311 (1990).
6. M. El–Maazawi, R. Maboudian, Z. Postawa and N. Winograd, Rev. Sci. Instrum. 43, 12078 (1991).
7. H. D. Hagstrum, Phys. Rev. 96, 336 (1954).
8. J. H. Lin and B. J. Garrison, J. Vac. Sci. Technol. A 1, 1205 (1983).
9. R. T. Williams, Radiat. Eff. and Defects in Solids 109, 175 (1989).
10. T. A. Green, G. M. Loubrier, P. M. Richards, N. H. Tolk and R. F. Haglund, Jr. Phys. Rev. B 35, 781 (1987).
11. M. L. Hu, D. Grischkowsky and A. C. Balant, Appl. Phys. Lett. 39, 703 (1981).
12. M. Szymonski, P. Czuba, T. Dohnalik, L. Jozofowski, A. Karawajczyk, J. Kolodziej, R. Lesniak and Z. Postawa, Nucl. Instrum. Meth. B 48, 534 (1990).
13. W. Husinsky and R. Bruckmuller, Surf. Sci. 80, 637 (1979).
14. M. Szymonski, J. Rutkowski, A. Poradzisz, Z. Postawa B. Jorgensen, in "Springer Series in Surface Science", Vol. 4, Springer–Verlag, Berlin, Heidelberg, New York, (1984) p. 160.
15. N. Winograd, D. E. Harrison and B. J. Garrison, Surf. Sci. 78, 467 (1978).
16. Z. Postawa, P. Czuba, A. Poradzisz and M. Szymonski. Radiat. Eff. and Defects